Energy Resilience Modeling for Smart Houses

Hamed Ghasemieh*, Boudewijn R. Haverkort*, Marijn R. Jongerden* and Anne Remke*†
*Design and Analysis of Communication Systems
University of Twente, Enschede, The Netherlands
Email: [h.ghasemie, b.r.h.m.haverkort, m.r.jongerden, a.k.i.remke]@utwente.nl
† University of Münster, Münster, Germany
Email: anne.remke@wwu.de

***Abstract*—The use of renewable energy in houses and neighbourhoods is very much governed by national legislation and has recently led to enormous changes in the energy market and poses a serious threat to the stability of the grid at peak production times. One of the approaches towards a more balanced grid is, e.g., taken by the German government by subsidizing local storage for solar power. While the main interest of the energy operator and the government is to balance the grid, thereby ensuring its stability, the main interest of the client is twofold: the total cost for electricity should be as low as possible and the house should be as resilient as possible in the presence of power outages. Using local battery storage can help to overcome the effects of power outages. However, the resulting resilience highly depends on the battery usage strategy employed by the controller, taking into account the state of charge of the battery. We present a Hybrid Petri net model of a house (that is mainly powered by solar energy) with a local storage unit, and analyse the impact of different battery usage strategies on its resilience for different production and consumption patterns. Our analysis shows that there is a direct relationship between resilience and flexibility, since increased resilience, i.e., reserving battery capacity for backup, decreases the flexibility of the storage unit.**

I. Introduction

Over the last decade, we have seen an increasing amount of locally generated energy in households. The decrease in costs of photovoltaic (PV) panels, and governmental subsidies for solar energy has lead to a huge increase of distributed generation with PV-systems. Especially in Germany, the national government has been very successful in increasing the number of installed PV-power. Even though this provides a large contribution to the country's generation of renewable energy, the large increase of distributed generation has its drawbacks as well, as it leads to enormous production peaks. At sunny days the amount of generated solar energy becomes so large that it is a serious thread to grid stability.

These problems can be overcome through grid balancing, which ,however, requires the possibility to store locally generated energy. The German government, for example, subsidises investments in battery storage for solar energy. Local storage reduces the amount of power that is exported to the grid at peak production times, hence, leads to a better balanced and more stable grid.

On the other hand, investing in local storage facilities also allows to increase the resilience of smart houses and neighbourhoods, since the local storage can provide back-up power to isolated units in case of grid failures. Commercial systems with both of these functionalities, increasing local usage and providing back-up power, are available on the market, e.g, Nedap's PowerRouter [1] or SMA's Sunny Island [2]. Although the back-up power may not always serve as an uninterrupted power supply (UPS), in the context of smart houses it is already very important to ensure that power is available after a short switching period.

This paper presents a hybrid Petri net model of a smart house with local storage, adaptable production and demand patterns per hour and a battery management unit that allows to implement different strategies. As a quantitative measure of resilience that focuses on the effect of interruptions over time, we analyse the so-called *survivability* [3] of the smart house, given the presence of a power outage. The survivability specifies the probability that the house can be continuously powered from the locally produced and stored energy during a grid failure. Clearly, this probability highly depends on the current production and demand profile, the time of day the failure occurs, and the duration of the failure.

We analyse a wide range of scenarios with realistic production and demand patterns, (obtained from [4] and [5]) and three different battery management strategies. Our analysis shows a clear trade-off between the improved resilience against grid failure on the one side and flexibility for balancing purposes on the other.

Next to obtaining interesting measures for a system with a high social and economical importance, the contribution of this paper also lies in the application of state-of-the-art modelling and analysis techniques for Stochastic Hybrid Models (SHMs), i.e., models that combine discrete, continuous and stochastic variables. Note that the formalism we use, forms a highly restricted subclass of SHMs, which has already proven useful in the past. Due to these restrictions, it is possible to compute exact transient measures of interest with highly efficient algorithms and to analyse a wide set of scenarios with many different parameter choices, e.g., for the time point of the grid failure.

The rest of the paper is structured as follows. In Section II an overview of related work is given. In Section III we describe the system we will analyse. Section IV describes the modelling formalism of hybrid Petri nets, and we describe the system under study in this modelling formalism in Section V. Section VI provides and discusses the results of our analysis for different scenarios, both with and without grid failure. We conclude the paper in Section VII.

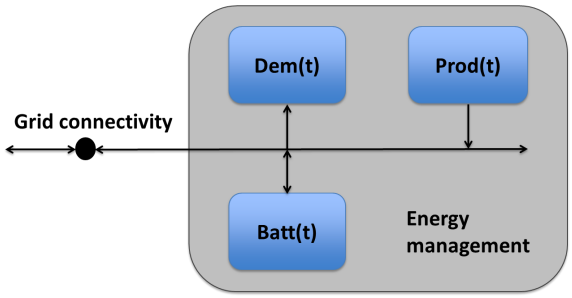

Fig. 1. Block diagram of the system.

II. Related work

Smart grids are highly complex systems [6], controlled by an ICT network that is used to exchange information. The electricity grid consists of multiple voltage levels and generated electricity is fed in on different voltage levels, where transformers convert energy between voltage levels. In order to model the stability of the grid, electricity demand, power generation, grid losses, the capacity and loss in transformers, as well as renewable generation need to be taken into account [7]. Most work on modelling of smart grids focuses on optimization [8], [9], stability issues [10] or presents relatively simple Petri net models for dependability assessment [11].

Work specifically on grid resilience has been done in the past, however, thereby primarily focussing on the resilience of the high- and medium-voltage grid. In these studies, the impact of failures, e.g., due to thunderstorms, is studied in terms of the (expected) energy not supplied per unit of time, see, e.g., [12], [13]. The proposed models are primarily based on Markov chains, stochastic activity networks and Markov reward models; numerical analysis or simulation is used for evaluation purposes. The proposed models for grid resilience have a discrete state space and, typically, the expected energy not supplied (per unit time) is computed (or estimated) using a time-scale decomposition. A recent overview of this type of work, but also related work for the gas and water infrastructure can be found in [14]. The recent work of Hartmanns and Hermanns focusses on the impact of large-scale photovoltaic generation on the stability of the grid [10].

All these works take the standpoint of the grid operator and/or the energy supplier. Instead, in this paper we focus on the viewpoint of the end-user, in that we study the continuity of energy delivery to end-user appliances (in homes or in small offices or companies), irrespective of what happens exactly in the grid. In our modelling approach, the grid is just seen as a source of energy delivery, albeit with possible interruptions. Our approach allows us to study the impact of grid disruptions, for whatever reason, on end-user perceived energy delivery continuity, and how we can improve the perceived continuity of energy delivery by installing smart local storage. The models we use are truly stochastic hybrid models, in that they combine deterministic events with probabilistic events on a mixed discrete/continuous state space. To the best of our knowledge, this has not been reported before.

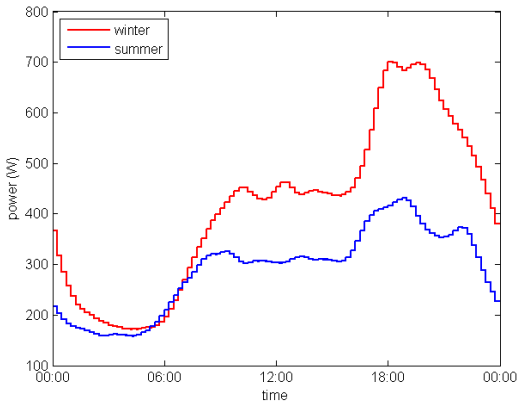

Fig. 2. Summer and winter day demand profile, as defined by EDSN [4].

III. System set-up

The system we consider is a house with PV-panels for energy generation and a battery for energy storage. Figure 1 shows a block diagram of the scenario. The demand within the house is presented by a time-dependent function $Dem(t)$. The locally generated energy is given by the function $Prod(t)$. The function $Batt(t)$ describes how the battery is charged and discharged. At any point in time, the demand has to be served from either the local production, the battery, or the grid. The *energy management system* within the house decides on when to use which energy source. In what follows, we address these four functions in detail.

A. Demand

The energy demand of a household depends on the time of day, and the day of the year. In the Netherlands, the electricity demand will typically be high in winter, and lower in summer. One could use a smart meter to measure a demand profile for a given household. In this research, we use a standardized demand profile supplied by EDSN [4]. EDSN creates standard demand profiles for all possible type of grid connections. These profiles give, for a full year, the average power drawn with a 15 minute granularity. Figure 2 gives an example of a summer and winter day profile for a household connection with a single meter and a total yearly demand of 3000 kWh.

B. Production

The energy generation by the PV-panels, of course, mainly depends on the local weather. In general, the production will by high in summer and lower in winter. But large variations may occur on a day to day basis, since sunny days may be followed by days with many clouds. With weather data, specifically solar irradiation data, supplied by weather agencies, one can construct local generation profiles. For the Netherlands, the Royal Netherlands Meteorological Institute provides historical data of all its weather stations [15]. The irridiation data still needs to be converted to energy production. The conversion depends on the size, location, orientation and efficiency of the installed PV-system. On the internet, tools like the one by PVWatts [5] directly can provide a generation profile with one hour granularity based on the PV-system specifications. Figure 3 shows four day profiles, two days in summer and

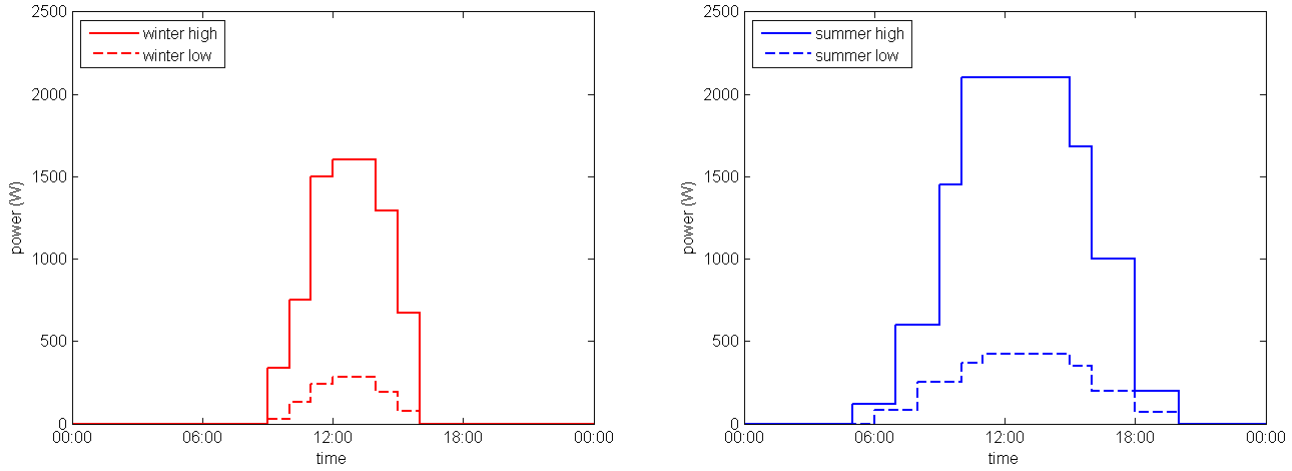

(a) Winter (b) Summer

Fig. 3. Production profiles of (a) winter and (b) summer days obtained from PVWatts [5]. For both seasons a high and low production day are given.

two days in winter. For both seasons a profile of a sunny day with high production and a profile of a cloudy day with low production are shown.

C. Battery

The battery has two main functions. First, when the grid is available, it can be used for energy balancing. By smartly charging the battery with the locally generated energy and discharging at times when the local generation is low, the impact of the household on the grid can be reduced. The second function of the battery is to provide back-up power when the grid fails.

Commercially available solutions that combine a PV-generation with a battery (see [2], [1]) use lead-acid or lithium-ion batteries. In home applications the usable capacity will be up to 5 kWh. The actual nominal battery capacity will be much higher, since the batteries are never used for 100%, to increase their cycle life, i.e., the number of charge discharge cycles until the battery is depleted. Lead-acid batteries are typically discharged for only 50% of their full capacity, and Li-ion Batteries for 70 to 80%.

The partial usage of the battery reduces the impact of the non-linear properties such as the rate-capacity effect [16]. Even at high discharge currents it will be possible to discharge the battery for the limited amount of energy. This makes that we can approximate the battery with an ideal storage system without introducing large errors.

D. Energy management system

The energy management system decides when to charge and when to discharge the battery. Three strategies are considered in this study. In all three strategies the demand is with priority powered by the local production. When the local production is smaller than the demand, the battery is used if possible. Only when really needed, the grid is used to supply the energy to the demand. The following strategies are considered:

i. *Greedy*: The battery is always discharged for its full available capacity. The battery is charged only with locally produced energy.
ii. *Smart*: When the grid is available, the battery is never fully discharged. It is discharged only to a predefined state of charge, denoted SoC_1. Part of its usable energy is kept as back-up energy. This energy is available when a grid failure occurs. Like the *Greedy* strategy, the battery is charged only with locally produced energy.
iii. *Conservative*: Like in the *Smart* strategy, the battery is discharged only to the level of SoC_1 when the grid is available. However, when this state is reached, the grid is used to partially recharge the battery with a fixed rate I, to SoC_2. This results in additional back-up energy, when a grid failure occurs.

IV. Hybrid Petri nets

This section intuitively recalls the modelling formalism of Hybrid Petri nets (HPnGs). Like many other Petri net models, also HPnGs are user friendly and close to real life applications. Hence, this section stresses the graphical representation of HPnGs, and refers to [17], [18], for a detailed discussion of the syntax and semantics.

A. Modelling formalism

An HPnG model is designed to describe real systems containing both discrete and continuous variables, combined with stochastic behaviour. It consists of three main sets of components: (i) *places* (discrete and continuous), which model different modes of the system; (ii) *transitions*, which allow changes between different modes of the system; and finally (iii) *arcs* (connecting places and transitions), which determine how the other two sets are related to each other, i.e, how a transition between different modes of the system can take place. Each of these three sets contains different types, with graphical representations as illustrated in Figure 4.

The set of **places**, $\mathcal{P}$, contains two disjoint sets of *discrete* ($\mathcal{P}^D$) and *continuous* ($\mathcal{P}^C$) places. The former keeps track of

discrete variables of the system, e.g., the number of spare parts, and the latter contains the continuous state of the system, e.g., the amount of fluid in a container. A discrete place may contain a number of *tokens*, while a continuous place is assigned with a real number, representing the level of fluid residing in it. We later refer to the content of places as the *marking* of the system.

Transitions will trigger a change in the state of the system, i.e., they may change the marking of place(s), provided that all the required resources are available. In this case we say that the transition is *enabled* and may *fire*. The set of transitions, $\mathcal{T}$, consists of four disjoint sets. Immediate ($\mathcal{T}^I$), deterministically timed ($\mathcal{T}^D$), and generally timed ($\mathcal{T}^G$) transitions, all referred to as discrete transitions, are responsible for changing the discrete part of the system (the marking of the discrete places), whereas continuous transitions ($\mathcal{T}^C$) change the marking of continuous places. An immediate transition will fire at the very moment it is enabled, and a deterministic transition will fire at a specific time after it has been enabled. Each deterministic transition, T_i^D, is associated with a clock c_i, which evolves with drift $dc_i/d\tau = 1$, if the transition is enabled. When a clock reaches its firing time, transition T_i^D fires, and the clock is reset to zero. A general transition will fire according to an arbitrary probability distribution after it has been enabled. More specifically, a general transition T_k, associated with the probability distribution $g_k(s)$, fires with probability $\int_{\tau}^{\tau+\Delta\tau} g_k(s)ds$, in the time interval $[\tau, \tau + \Delta\tau]$. Note that the execution policy of the general transitions, i.e., their enabling/disabling semantics, is of type *race with age memory*, i.e., the clock of a general transition is preserved upon disabling and resumed with enabling [19]. The total time a general transition is enabled before it fires is drawn independently from its respective probability distribution. There may be a dependence between the actual time of firing due to the time transitions have been disabled, which depends on the structure of the Petri net.

Continuous transitions, as their name suggests, will fire continuously, according to an assigned rate, and will thereby change the content of continuous places, provided that they are enabled. Moreover, a continuous transition can be *static* or *dynamic*, meaning that it will either fire with constant *nominal rate*, or its rate can dynamically depend on the rates of other static continuous transitions.

The set of **arcs**, $\mathcal{A}$, characterizes how transitions and places are related to each other. Discrete arcs, $\mathcal{A}^D$, connect discrete places to transitions, in the following way. If a transition fires, it will remove tokens from places connected to it via input arcs, and add tokens to the places that are connected via output arcs. The number of tokens being removed or added are determined by the weights assigned to the arcs. Continuous arcs, connect continuous places and transitions. Therefore, when a continuous transition fires, it will remove content of its input places and add to the content of its output places, with a specific rate assigned to the transition. The set of guard arcs, $\mathcal{A}^G$, connects discrete transitions to both discrete and continuous places. These arcs ensure that a transition is only enabled in case the number of tokens (in case of a discrete place) or the amount of fluid (in case of a continuous place) fulfills a certain condition that is specified on the guard arc.

In the HPnG modelling formalism, we associate with each continuous place a lower and upper boundary. Conflicts between continuous transitions occur when a continuous place reaches one of these boundaries. To prevent overflow, the fluid input has to be reduced to match the output, and to prevent underflow the fluid output has to be reduced to match the input. This means that the rates of inputs/outputs transitions have to be adapted. The newly adapted rates of continuous transitions are called *actual rates*, in contrast to their preassigned nominal rates. The rate for each transition is determined based on the *priorities* and *shares* assigned to the arcs, connecting continuous transitions and the place. This process is called *rate adaptation*. For further details on this, we refer to [20].

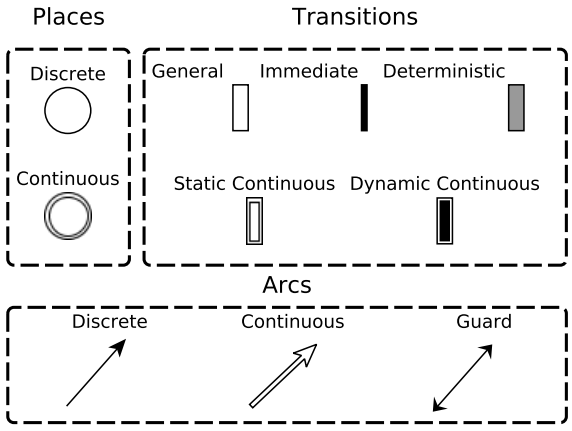

Fig. 4. Graphical representation of primitives of HPnG.

B. State of the system

Markings, i.e., the content of places, are collected into two vectors, the discrete marking $\mathbf{m} = (m_1, \ldots, m_{|\mathcal{P}^D|})$ and the continuous marking $\mathbf{x} = (x_1, \ldots, x_{|\mathcal{P}^C|})$. The initial marking is composed of a discrete part $\mathbf{m}_0$ that describes the initial amount of tokens in all discrete places and a continuous part $\mathbf{x}_0$ that describes the initial amount of fluid in all continuous places.

The overall *state* of an HPnG is defined by $\Gamma = (\mathbf{m}, \mathbf{x}, \mathbf{c}, \mathbf{d}, \mathbf{g})$, where the vector $\mathbf{c} = (c_1, \ldots, c_{|\mathcal{T}^D|})$ contains a clock c_i for each deterministic transition that represents the time that T_i^D has been enabled. When a transition is disabled the clocks do not evolve, but the clock value is preserved until the transition is enabled again. Clocks are only reset when the corresponding deterministic transition fires. Vector $\mathbf{d} = (d_1, \ldots, d_{|\mathcal{P}^C|+|\mathcal{T}^D|})$ indicates the drift of all continuous variables. For continuous places it indicates the change of fluid per time unit, and for deterministic transitions it is the clock drift, one for enabled and zero for disabled transitions, respectively. Note that even though the vector $\mathbf{d}$ is determined uniquely by $\mathbf{x}$ and $\mathbf{m}$ in combination with the condition of guard arcs, it is included in the definition of a state for the ease of analysis. Finally, $\mathbf{g} \in \mathbf{N}$ indicates whether the general transition has already fired, or not.

V. Hybrid Petri net model for a smart house

In this section, we present a Hybrid Petri net model for a smart house, corresponding to the block diagram presented

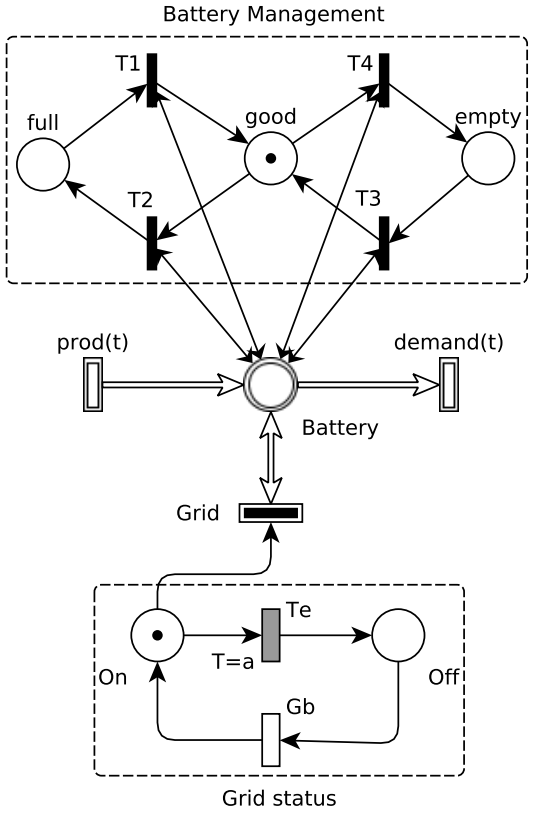

Fig. 5. HPnG model of a resilient house.

in Figure 1. Using this model, we will be able to compute measures of interest, like the amount of energy produced from renewable energy, the amount of energy that has to be taken from the grid and the survivability of the system in the case of a power outage.

A. Hybrid Petri net model

Figure 5 shows an abstraction of the HPnG model of a smart house; it consists of three parts (from top to bottom): (i) the battery management system, (ii) the model of the battery together with production and demand, and (iii) the model for the status of the grid.

The battery is modelled as a continuous place with overall capacity B, its current state of charge changes with the *time-dependent* production $prod(t)$ and demand $demand(t)$. Recall that we assume an ideal battery, where the change of charge is always linear. For simplicity of representation in the figure, we have collapsed the deterministic rates representing the different production and demand rates during the day into the time-dependent rates $prod(t)$ and demand $demand(t)$. Note that they represent in total up to 18 different rates that have been used in the model to closely model the production and demand at different times of a single day.

In case the local generation produces more energy than is used and can be stored in the battery, this energy can be forwarded to the grid. Similarly, in case there is not enough local energy available to power the house, energy is taken from the grid into the house. However, this is only possible when the grid is operational, i.e., a token is currently in place *On*. For simplicity, the interaction between the battery and the grid is represented by a bidirectional continuous arc.

The grid failure is modelled as a deterministic transition, which can be parametrized through variable a. This allows us to analyse the impact of different times of failure on the survivability. The firing of this deterministic transition moves the token to place *Off* and the house is then practically isolated from the grid. The grid returns from its failure according to a stochastic repair distribution that can be chosen freely.

The *Battery Management Unit* controls the flow of power between the local generation, the battery, the house and the grid. In case more energy is needed than is produced from the local generation, it decides whether to take the additional power from the grid or from the battery, depending on the battery management strategy used. The model distinguishes between three states of the battery, it can either be *full*, *good* or *empty*, where the state *empty* can be interpreted relative to the overall capacity of the battery B. The transitions T_i for $i \in \{1, 2, 3, 4\}$ coordinate the change of state via test arcs that enable the firing of transition T_i according to some threshold that is compared to the available capacity of the battery. Note that whenever the system is in state *good*, no energy exchange with the grid takes place. However, depending on the battery management strategy it represents *different* intervals of state of charge.

Recall that we will analyse the impact of three different battery management strategies: *Greedy*, *Smart* and *Conservative*. These can all be encoded in the model of the battery management unit through different thresholds that control that state of the battery (*full*, *good* and *empty*). Also, the dynamic continuous transition *Grid* plays an important role in implementing the strategies. In all cases when the battery is *empty* this transition imports the energy that is missing to power the house, i.e., the difference between production and demand, but for strategy *Conservative* it additionaly imports energy that is used to charge the battery at a fixed rate I. Note that the concept of dynamic continuous transitions allows to summarise this behaviour in a single transition.

All thresholds are chosen relative to the overall capacity of the battery B. The thresholds for transition T_1 and T_2 are used to check whether the current state of charge is smaller and greater or equal to B, respectively. The threshold for T_4 is used to check whether $B \leq SoC_1$ and the threshold for T_3 checks whether $B > SoC_1$ for strategies *Greedy* and *Smart*, and checks whether $B > SoC_2$ for strategy *Conservative*. The precise values for the state of charge SoC_1 and SoC_2 will be presented later. Note that in order to avoid Zeno behaviour[1] in the model evolution, all transitions T_i are timed transitions that fire with a small delay ϵ.

The simultaneous inflow and outflow of energy from the battery in the model is, of course, in reality not possible. One cannot charge and discharge a battery at the same time. In practice, the simultaneous production and demand will bypass the battery. However, the presented model will yield the same results with respect to the chosen measures of interest.

[1]That is, infinitely many transitions in near zero time.

B. Model evaluation and measures of interest

Recently, efficient analysis algorithms have been developed for the restricted sub-class of HPnGs that contain only one general transition that is allowed to fire just once, i.e., there is exactly one random variable present in the model. It is then possible to compute the transient probability to be in a state with a certain property [17], but it is also possible to specify more complex properties, using the logic STL [21]. For example, the following timed until formula:

$$\texttt{survivability} = \texttt{battery\_up}\ \mathcal{U}^{[\texttt{a},\texttt{a}+\texttt{t}]}\texttt{grid\_on},$$

can be used to specify the survivability for so-called *Given the Occurrence Of Disaster* (GOOD) models, where a failure (the power outage) is assumed to occur at a certain time a. The above formula then specifies that power is available from the battery continuously until the grid is back on within t time units. For finite values of t, algorithms for model checking such formulae have also been presented in [21] and have been implemented in the FluidSurvivalTool [22], that allows to import the model as textual input and then provides a graphical user interface to specify and analyse the properties of interest.

Due to the efficiency of our model checking algorithms, it is possible to compute the probability to be in a survivable state very quickly for a wide range of failure times a, so that parametric studies can be easily performed.

VI. Results

In this section we present the results of our analysis. First, we study the system without a grid failure, in order to analyse the basic behaviour of the battery management strategies. Subsequently, we analyse the impact of a grid failure on the smart house.

A. Parameter choices

In our analysis we consider 4 different configurations of demand and production profiles: 2 summer and 2 winter configurations. The demand profiles are based on the EDSN profiles shown in Figure 2, for a total yearly demand of 3000 kWh. However, to reduce the computational complexity for the hybrid Petri net model, we use a more coarse grained approximation. The approximation profiles are given in Figure 6.

Similarly, the production profiles shown in Figure 3, obtained from PVWatts, have been approximated, see Figure 7. The PVWatts profile is computed for a system located in Amsterdam with twelve 250 Wp (Watt peak) solar panels (3 kWp total), facing south with a 45 degree tilt. The system losses, and all advanced parameters have been kept to the default values. These input values result in a yearly production of approximately 2750 kWh.

For the 4 combinations of production and demand, the three battery management strategies have been evaluated for

TABLE I. Choice of the threshold levels

strategy	SoC_1	SoC_2
greedy	0	0
smart	$0.3C_u$	$0.3C_u$
conservative	$0.3C_u$	$0.5C_u$

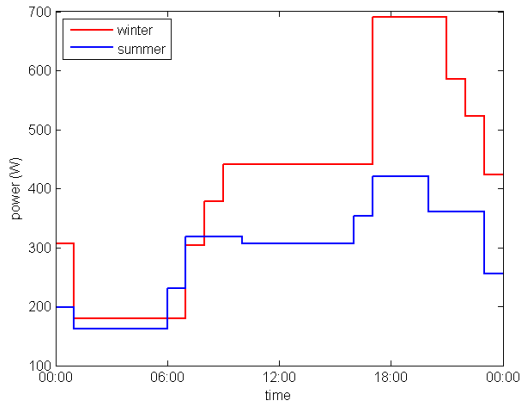

Fig. 6. Approximation of the summer and winter day demand profiles.

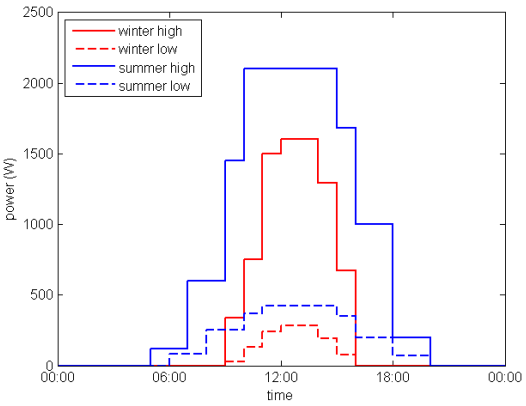

Fig. 7. Approximation of the summer and winter day production profiles.

varying usable battery capacities (C_u), ranging from 500 Wh to 3000 Wh. Table I gives the choice of the levels of SoC_1 and SoC_2 in the three strategies. The rate at which the battery is charged from the grid in the *Conservative* strategy is set to $0.2C_u/8$. Thus, the battery will be charged by the grid from $0.3C_u$ to $0.5C_u$ in 8 hours. The battery is charged by the grid in such a relatively low rate in order to reduce the additional load on the grid, and to prevent a large number of partial charge-discharge cycles during the night.

B. Results without grid failure

In order to get a first idea of how the battery management strategies work, and to see what the impact of the system on the grid is in the different production and demand scenarios, we first study the case that no grid failure occurs. This is done through a Matlab-based simulation of the Petri net model (as presented in Section IV) without the *Grid Status* part. Note that in this case the model evolution is fully deterministic.

The scenario we use is a summer day with a high production profile combined with a summer demand profile. The usable battery capacity has been set to 2500 Wh. This scenario has been chosen since it clearly shows all possible energy flows. The simulation starts at midnight with a full battery, and covers three full days. For each hour, we compute the

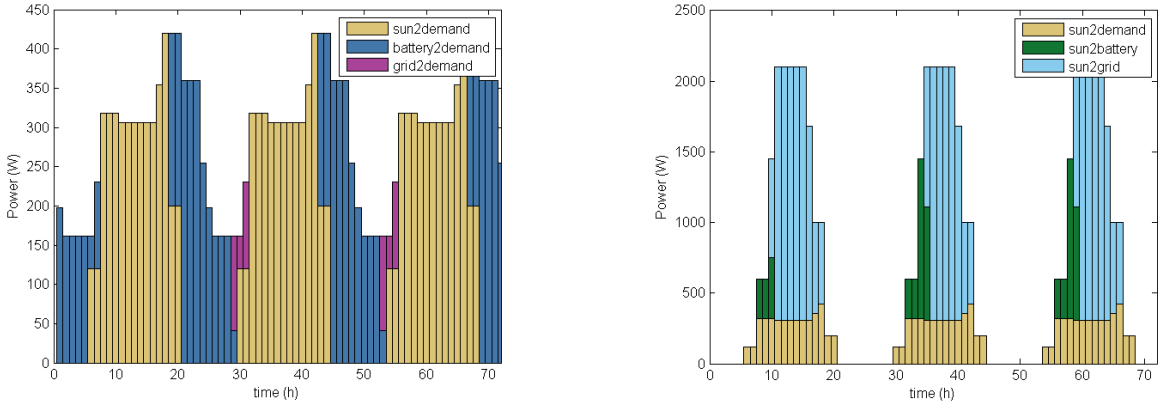

(a) Demand (b) Production

Fig. 8. Distribution of the power of the sources to supply the energy to the demand (a), and the distribution of the generated power over the destinations demand, battery and grid (b), for the *Greedy* management strategy.

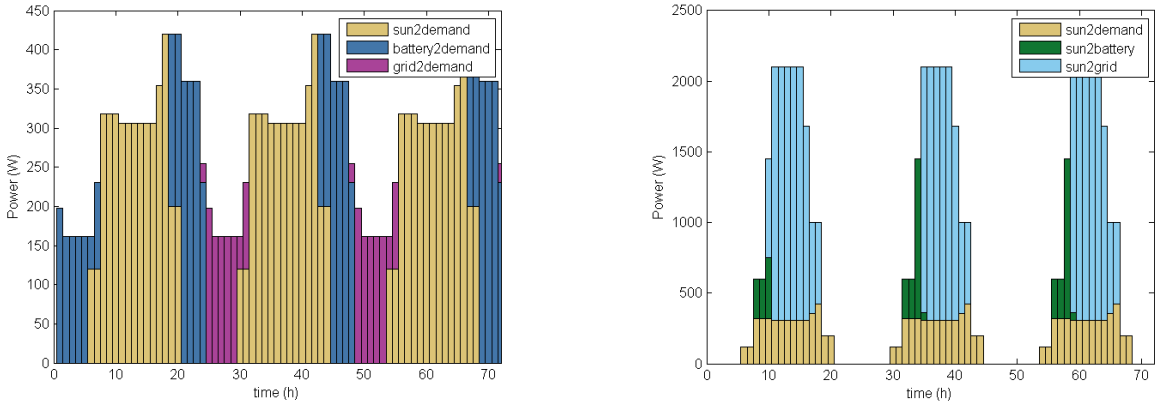

(a) Demand (b) Production

Fig. 9. Distribution of the power of the sources to supply the energy to the demand (a), and the distribution of the generated power over the destinations demand, battery and grid (b), for the *Smart* management strategy.

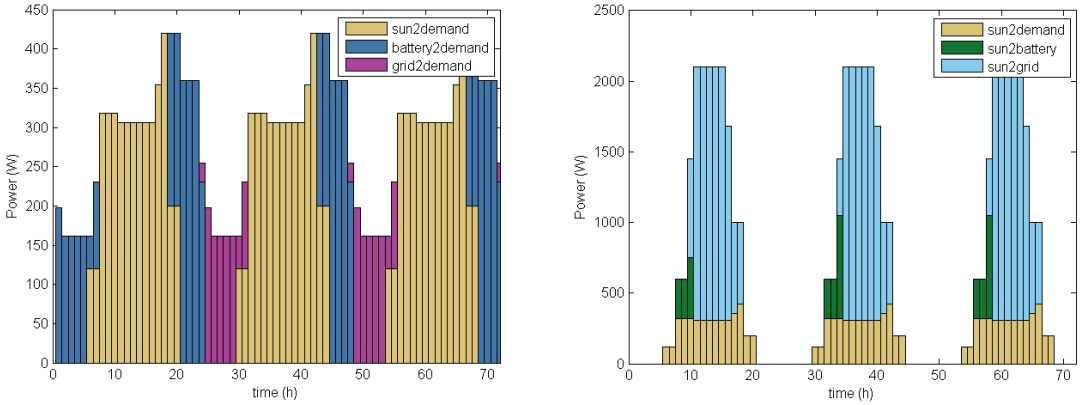

(a) Demand (b) Production

Fig. 10. Distribution of the power of the sources to supply the energy to the demand (a), and the distribution of the generated power over the destinations demand, battery and grid (b), for the *Conservative* management strategy.

energy flowing from each power source (that is, PV, battery and grid), to each destination (that is, demand, battery and grid). Figure 8 shows the results of the *Greedy* strategy. Figure 8a shows the demand profile, and how much energy is supplied by the different sources. The surface area under the power profile represents the energy in Wh. Similarly, Figure 8b, gives the distribution of the produced energy over the different destinations.

Since the system starts at midnight with a full battery, the demand is first supplied with energy from the battery. In the morning the PV-system starts up, and takes over the energy supply from the battery. During the day, enough energy is available to charge the battery. In the evening when the sun sets, the battery again takes over. At the end of the second night the battery is fully discharged and the grid is used to supply part of of the energy. The third day is the same as the second.

Figures 9 and 10 show the results for the smart and conservative strategy, respectively. We see that now the grid is used more to supply energy to the demand, than in the greedy strategy. The reason is that the battery is discharged only to an SoC of $0.3C_u$. This is also reflected in that less energy is needed to charge the battery from the PV-system. Even less energy of the PV-system is used to charge the battery in the conservative strategy. The reason is that the battery is partially charged by the grid during the night.

C. Survivability results

In the following we consider the impact of a grid failure on the smart house for all three battery management strategies and the four production profiles as discussed in Section VI-A. The grid may fail at different times of the day and comes back after a random repair time, that is distributed according to a folded Normal distribution, with average 2 and standard deviation of 1 (hour). Power outage times are monitored and reported by the Council of European Energy Regulators (CEER). In their recent benchmarking report on the continuity of electricity supply [23], one can see that the unplanned system average interruption duration index (SAIDI) differs largely per country, in 2012 ranging from only 10 and 14.5 minutes for, respectively, Luxembourg and Denmark, to as much as several hundreds of minutes in the Baltic states and Poland and Malta. The unplanned system average interruption frequency index (SAIFI) is well below 1 for some countries (like Luxembourg, the Netherlands and Denmark) and ranges to, for example, 2.33 for Italy and 2.99 for Slovenia. We did not manage to obtain any data about individual outage times, that is, per outage event, let alone distributional information on these, even though we contacted several grid operators directly about this.

We show the survivability of the system, that is, the probability that the house can be powered continuously in the presence of a power outage, for battery sizes between 500 and 3000 Wh. We start with a full battery at midnight (which corresponds to time 0 in the figures). These results are computed using the FluidSurvivalTool [22] and the full version of the model presented in Section V.

1) Greedy: Figure 11 presents the survivability of the system, when the *Greedy* strategy is used for the four different production profiles. The time of failure is depicted on the x-axis and the probability that the system is survivable, that is, the probability the demand can be fulfilled without interruptions, on the y-axis. The time of failure (on the x-axis) corresponds to the firing time of the failure transition T_e in the HPnG model and does not represent the transient evolution of time. Clearly, the state of charge of the battery changes over time, hence, the time of failure has a direct impact on the survivability of the system.

In winter when the production is low the available energy from the battery is quickly consumed, since the *Greedy* strategy always first empties the battery before it imports energy from the grid. Together with the state of charge of the battery the survivability of the system drops rapidly, and as shown in Figure 11(a). Depending on the size of the battery, the probability that the system is survivable reaches zero for grid failures occurring between 5 to 15 hours. As the production in this setting is always lower than the demand, the battery will never be recharged on a winter day with low production. Hence, the system can not recover, once the battery has been drained.

The situation changes when the production is higher, e.g., on a sunny winter day. The results for this setting are shown in Figure 11(b) and one can see that the survivability is high after noon (12 p.m.), but drops in the evening between 7 p.m. and 9 p.m., depending on the size of the battery. The reason is that the larger production during a sunny afternoon allows to recharge the battery and a full battery provides the means to survive a power outage for a couple of hours. However, during the night and the early morning the battery is always empty due to the *Greedy* strategy, hence, the probability to survive an outage at these times is zero. The described pattern repeats for consecutive days with this setting. The differences with the first 12 hours are due to the chosen initial condition of the full battery which increases the probability to survive in the beginning.

In summer when the production is low, e.g., on a rainy day, one can see in Figure 11(c) that the initial transient phase takes a full day. During this first day the survivability highly depends on the size of the battery, since a larger capacity provides more backup in case of a grid failure. However, after the battery has been emptied once (after the first 24 hours) one can see that the survivability is independent of the battery capacity. The reason is that although the battery is charged during the day, due to the low production, it is never charged above 600 Wh. Hence, additional battery capacity does not have an advantage with respect to the survivability.

On a summer day with a high production (Figure 11(d)) the start-up phase is much shorter, i.e., less than 10 hours. The reason is that the production is so high that an empty battery is quickly charged in the morning. It is interesting to see that in this setting, with the highest battery capacity of 3000 Wh, the system is survivable with probability one for all considered failure times. With the battery of 2000 Wh the system is not survivable for a couple of hours during the night. Hence, in this setting it is preferable to have a larger battery, while on a summer day with a low production the additional capacity does not increase the survivability in the long run.

Overall, the *Greedy* strategy results in a poor survivability

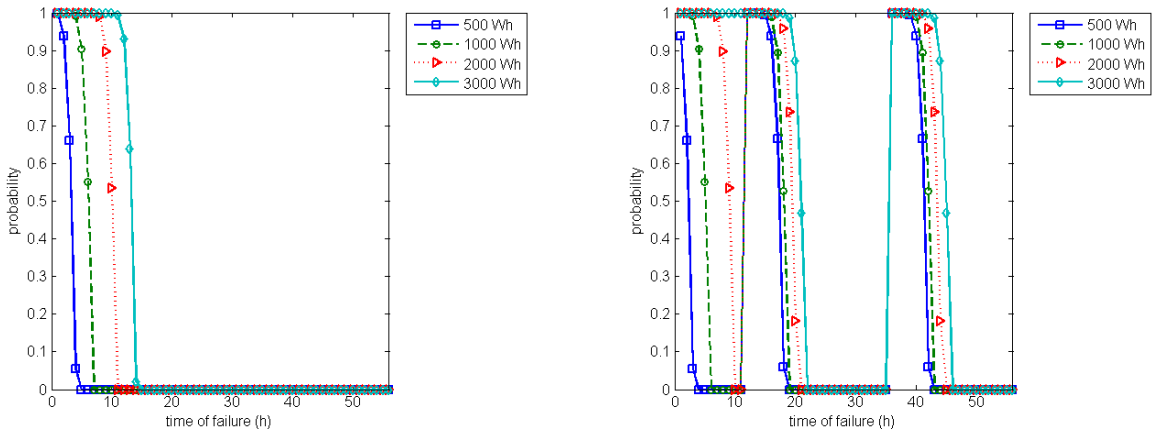

(a) Winter low production

(b) Winter high production

(c) Summer low production

(d) Summer high production

Fig. 11. Probability of surviving a grid failure as function of the time that the failure occurs for the *Greedy* strategy. The following four scenarios are considered, (a) winter day with low production, (b) winter day with high production, (c) summer day with low production, and (d) summer day with high production.

for three out of four production profiles, i.e., with the exception of a summer day with high production. In all other cases the complete draining of the battery leads to a zero probability to survive a power outage for large parts of the day. In the following we will look at the two remaining strategies, *Smart* and *Conservative*, for the two settings *Winter low* and *Summer high* to contrast the impact of the production profiles on the battery management strategies.

2) Smart: Figure 12 shows the survivability of the system when the *Smart* strategy is used. Recall that this strategy never drains the battery completely while the grid is available and always reserves 30% of the battery capacity to survive power outages. On a winter day with low production, as depicted in Figure 12(a), the survivability highly depends on the overall capacity of the battery. With this strategy the largest battery ensures a survivability of at least 70% for failures occurring at all times of the day, which is a large improvement with respect to the greedy strategy, where the survivability was zero, once the battery had been drained. When a smaller battery, e.g., 500 Wh, is used, the survivability drops to 10% during the night, which is clearly very low. This figure also exhibits a start-up phase, which is, however, rather small (less then 10 hours), after which a pattern repeats with a high survivability during the day and a dip during the evening hours. It is interesting to see that the survivability increases during the night even though the battery cannot be charged with local energy and will not be charged from the grid due to the strategy employed. This is due to the drop of the demand during the night, hence the system can survive longer on the remaining 30% battery capacity than during peak evening hours.

On a summer day with high production (cf. Figure 12(b)) the two largest batteries lead to a survivability of 100% for all potential failure occurrence times. For the two smaller batteries a pattern emerges after the initial start-up time of 10 hours, where the survivability is again high during the day, drops during the evening hours when the demand is very high and local energy is not available. During the night, the survivability then again increases due to the decreasing demand and returns to one as soon as the local generation produces energy again during the day.

When comparing the two strategies presented so far, the minimum survivability with the *Smart* strategy is, depending on the size of the battery, much better than when *Greedy* is

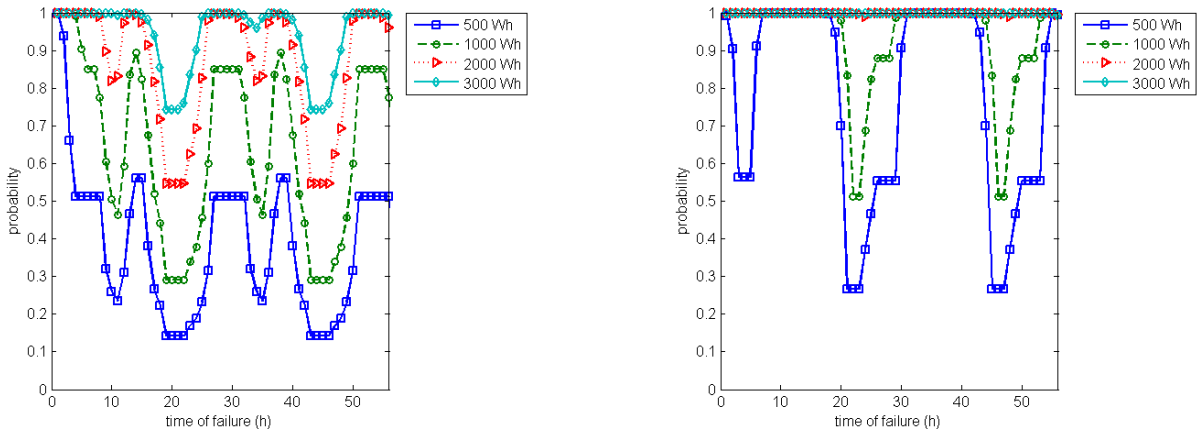

(a) Winter low production

(b) Summer high production

Fig. 12. Probability of surviving a grid failure as function of the time that the failure occurs for the *Smart* strategy. The following two scenarios are considered, (a) winter day with low production, and (b) summer day with high production.

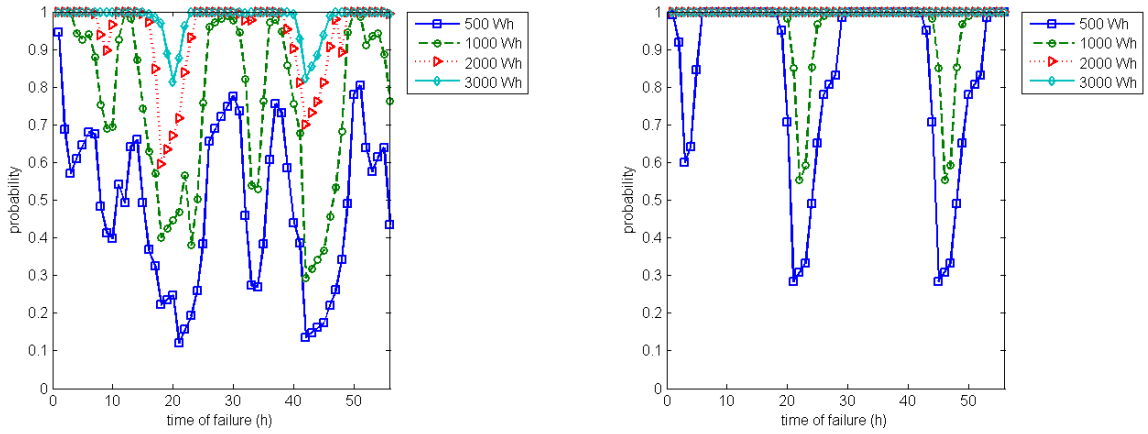

(a) Winter low production

(b) Summer high production

Fig. 13. Probability of surviving a grid failure as function of the time that the failure occurs for the *Conservative* strategy. The following two scenarios are considered, (a) winter day with low production, and (b) summer day with high production.

used. However, the time intervals *where* the survivability is not good remain the same.

3) Conservative: Finally, we also analyse the *Conservative* strategy, where the resilience of the system is increased by additionally charging the battery from the grid, when its state of charge is lower than the predefined threshold SoC_2. The resulting survivability is presented in Figure 13. Especially on a winter day with low production, the variability is much higher than in the other settings. The reason is that we observe a relatively high number of state changes between the states *good* and *empty* of the battery management unit. As soon as the state of charge is less than 30% of the overall battery capacity, the grid is used to power the house, and it *also* charges the battery until it reaches 50% of its capacity. If this occurs at a point in time where the local generation is still not producing enough energy, the house is then powered from the battery until again the state of charge hits the 30% threshold. Especially for smaller battery sizes these state changes occur relatively often since the difference between 30% and 50% state of charge is smaller. As a result of the large amount of variability in the system, also the results do not reveal a clear pattern for the different battery sizes.

On a summer day with high production, the survivability is much more regular, as shown in Figure 13(b). The start-up phase takes about 10 hours and we observe a survivability of one for the two large batteries and a minimum survivability of 30% and 55% for battery sizes 500 Wh and 1000 Wh, respectively, during the evening dips. When compared to the results for the *Smart* strategy one sees that the time intervals where the survivability is relatively low are much smaller for the *Conservative* strategy.

Overall one can conclude that achieving a high survivability is especially difficult on a winter day with low production. Having a larger battery only increases the survivability in this setting if one reserves backup power in the battery, that is only used in the case of a power outage. Additionally charging the

TABLE II. COMPUTATION TIMES AND MODEL SIZE.

strategy	production profile	total computation time (s)	max # regions	average # regions
greedy	winter low	23.7	573	182
	winter high	43.4	1384	402
	summer low	29.4	1099	239
	summer high	46.9	1410	401
smart	winter low	24.7	563	189
	winter high	51.2	1607	402
	summer low	36.6	1365	293
	summer high	60.3	1735	524
conservative	winter low	194.0	7188	1927
	winter high	129.5	5245	1331
	summer low	134.8	6106	1266
	summer high	109.5	5844	1021

battery from the grid in case of a low state of charge also improves the overall survivability and decreases the intervals of time where the survivability is low.

In contrast, on a summer day with high production the two large batteries are enough to ensure a survivability of 100% for the strategies *Smart* and *Conservative*, and even for *Greedy* the largest battery capacity ensures the same. One can conclude that in order to ensure a relatively high survivability, a smart house with the presented parameter settings would need a battery with at least a capacity of 2000 Wh and would employ at least strategy *Smart*. Note that, when the *Conservative* strategy is used, the thresholds SoC_1, SoC_2 and the additional charge from the grid have to be chosen carefully to reduce the number of state changes in the battery management unit, hence, to avoid cycling behaviour.

D. Computation times

To obtain the presented results, for each scenario, i.e., for each combination of production profile and battery management strategy, we have analyzed 248 different settings, each with a different overall battery capacity and failure time. For each of of these 248 combinations, a different so-termed Stochastic Time Diagram (STD) [24] needs to be generated and model checked in order to compute the required measure of survivability. The analyses have been performed on a machine equipped with a 2.0 GHz intel® CORE™ i7 processor and 4 GB of RAM.

The computations for each setting have taken at most half a second. To compute *all* 248 values for each scenario has taken a maximum of 194 seconds for the *conservative* strategy with a winter-low production profile (and less for all other scenarios). Moreover, the maximum number of generated regions for a STD has been slightly less that 7200. More details on the computation times and the number of generated regions are given in Table II.

VII. CONCLUSION

We have presented a Hybrid Petri net model that allows to analyse the effect of different battery management strategies on (i) how the locally generated energy is used, and (ii) how resilient the smart house becomes against power outages. We compute the so-called survivability, i.e., the probability that a house with local generation and battery storage can continuously be powered in case of a grid failure.

We use a dedicated Matlab simulator to analyse the distribution of the different power sources under the assumption that the grid is always operational. Note that this setting is fully deterministic. In the presence of a power outage the model can be analysed with techniques for Hybrid Petri nets that allow for one stochastic variable in the model. In the present paper this stochastic variable is used to model the time the grid needs to become operational again. Hence, the actual time point of repair of the grid is not explicitly visible in the results.

The impact of three different battery management strategies on the survivability of the house has been analysed. When comparing the three strategies *Greedy*, *Smart* and *Conservative*, we see that while *Greedy* allows to use the battery in the most flexible way, it also provides the lowest survivability. In contrast, when a certain percentage of the battery is only used in case of a power outage, the survivability increases considerably, but this part of the capacity cannot be used in a flexible way. This clearly shows the trade-off between using the battery for balancing purposes and providing back-up in case of a grid failure.

The *Conservative* strategy additionally charges the battery from the grid in case its current state of charge is below a certain level. While this leads to an even higher survivability, it also leads to many additional charge-discharge cycles, which in the end will not be beneficial for the battery itself.

The presented model uses an ideal battery model and in its current form does not take into account the cost for selling and buying power or the investment costs for a larger battery. Future work will see how a more accurate battery model, such as the Kinetic Battery Model [16], can be combined with stochastic failure and repair times and will also incorporate costs. This will allow us to better understand the trade-off between the investment costs for a large battery and the savings due to using mainly locally generated power.

ACKNOWLEDGMENTS

This work was realized as part of the e-balance project that has received funding from the European Union Seventh Framework Programme (FP7/2007-2013) under grant agreement n° [609132].

Anne Remke is partly funded by NWO, Veni grant 639.021.022, Dependability analysis of fluid critical infrastructures using stochastic hybrid models.

REFERENCES

[1] Nedap, "PowerRouter homepage," accessed April 2, 2015. [Online]. Available: http://www.powerrouter.com/en/

[2] SMA, "SMA homepage," accessed April 2, 2015. [Online]. Available: http://www.sma.de/en.html

[3] L. Cloth and B. Haverkort, "Model checking for survivability!" in *Proceedings of the Second International Conference on the Quantitative Evaluation of Systems (QEST 2005)*. IEEE, 2005, pp. 145–154.

[4] EDSN, "EDSN demand profiles," accessed April 2, 2015. [Online]. Available: http://www.edsn.nl/verbruiksprofielen/

[5] NREL, "PVWatts," accessed April 2, 2015. [Online]. Available: http://pvwatts.nrel.gov/index.php

[6] S. M. Amin, "Smart grid: Overview, issues and opportunities. advances and challenges in sensing, modeling, simulation, optimization and control," *European Journal of Control*, vol. 17, no. 56, pp. 547 – 567, 2011.

[7] H. Hermanns and H. Wiechmann, "Future design challenges for electric energy supply," in *Proceedings of the IEEE Conference on Emerging Technologies Factory Automation (ETFA 2009)*, 2009, pp. 1–8.

[8] V. Bakker, M. G. Bosman, A. Molderink, J. L. Hurink, and G. J. Smit, "Improved heat demand prediction of individual households," in *Proceedings of the first Conference on Control Methodologies and Technology for Energy Efficiency*. Elsevier, 2010, pp. 110–115.

[9] M. Welsch, M. Howells, M. Bazilian, J. DeCarolis, S. Hermann, and H. Rogner, "Modelling elements of smart grids enhancing the {OSeMOSYS} (open source energy modelling system) code," *Energy*, vol. 46, no. 1, pp. 337 – 350, 2012.

[10] A. Hartmanns and H. Hermanns, "Modelling and decentralised runtime control of self-stabilising power micro grids," in *Proccesdings of the 5th International Symposium Leveraging Applications of Formal Methods, Verification and Validation. Technologies for Mastering Change. (ISoLA 2012)*. Springer, 2012, pp. 420–439.

[11] B. Wang, M. Sechilariu, and F. Locment, "Power flow petri net modelling for building integrated multi-source power system with smart grid interaction," *Mathematics and Computers in Simulation*, vol. 91, no. 0, pp. 119 – 133, 2013.

[12] A. Avritzer, L. Carnevali, L. Happe, A. Koziolek, D. S. Menasché, M. Paolieri, and S. Suresh, "A scalable approach to the assessment of storm impact in distributed automation power grids," in *Proceedings of the 11th International Conference on Quantitative Evaluation of Systems, (QEST 2014)*. Springer, 2014, pp. 345–367.

[13] S. Chiaradonna, F. D. Giandomenico, and N. Murru, "On a modeling approach to analyze resilience of a smart grid infrastructure," in *Proceedings of the Tenth European Dependable Computing Conference (EDCC 2014)*. IEEE, 2014, pp. 166–177.

[14] A. Avritzer, L. Carnevali, H. Ghasemieh, L. Happe, B. R. Haverkort, A. Koziolek, D. Menasche, A. Remke, S. S. Sarvestani, and E. Vicario, "Suvivability evaluation of gas, water and electricity infrastructure," in *Proceedings of 7th International Workshop on Practical Applications of Stochastic Modelling (PASM 2014)*. Elsevier, 2014, pp. 1–20.

[15] KNMI, "Uurgegevens van het weer in nederland," accessed April 2, 2015. [Online]. Available: http://www.knmi.nl/klimatologie/uurgegevens/

[16] M. R. Jongerden and B. R. Haverkort, "Which battery model to use?" *IET Software*, vol. 3, no. 6, pp. 445–457, 2009.

[17] M. Gribaudo and A. Remke, "Hybrid Petri nets with general one-shot transitions for dependability evaluation of fluid critical infrastructures," in *Proceedings of the 12th IEEE International High Assurance Systems Engineering Symposium (HASE 2010)*. IEEE Computer Society, November 2010, pp. 84–93.

[18] H. Ghasemieh, A. Remke, and B. R. Haverkort, "Analysis of a sewage treatment facility using hybrid Petri nets," in *Proceedings of the 7th International Conference on Performance Evaluation Methodologies and Tools (Valuetools 2013)*. ACM, 2013, pp. 165–174.

[19] M. Ajmone Marsan, G. Balbo, A. Bobbio, G. Chiola, G. Conte, and A. Cumani, "The effect of execution policies on the semantics and analysis of stochastic Petri nets," *Software Engineering, IEEE Transactions on*, vol. 15, no. 7, pp. 832–846, 1989.

[20] R. David and H. Alla, *Discrete, Continuous, and Hybrid Petri Nets*. Springer, 2010.

[21] H. Ghasemieh, A. Remke, and B. R. Haverkort, "Survivability evaluation of fluid critical infrastructures using Hybrid Petri nets," in *Proceedings of the IEEE 19th Pacific Rim International Symposium on Dependable Computing (PRDC 2013)*. IEEE, 2013, pp. 152–161.

[22] B. F. Postema, A. Remke, B. R. Haverkort, and H. Ghasemieh, "Fluid Survival Tool: A Model Checker for Hybrid Petri Nets," in *Proceedings of MMB/DFT 2014*. Springer, 2014, pp. 255–259.

[23] CEER, "CEER benchmarking report 5.1 on the continuity of electricity supply, ref. c13-eqs-57-03," February 2014, accessed April 2, 2015. [Online]. Available: http://www.ceer.eu/

[24] H. Ghasemieh, A. Remke, B. Haverkort, and M. Gribaudo, "Region-based analysis of hybrid petri nets with a single general one-shot transition," in *Proceedings of the 10th International Conference on Formal Modeling and Analysis of Timed Systems (FORMATS 2012)*. Springer, 2012, pp. 139–154.